Structure of Er-O complexes in crystalline Si

F. d'Acapito*
INFM-OGG, c/o GILDA CRG-ESRF, Boîte Postale 220, F-38043 Grenoble, France

S. Mobilio†
Dipartimento di Fisica, Universitá Roma Tre, Via della Vasca Navale 84, I-00146 Roma, Italy

S. Scalese
CNR-IMM, Stradale Primosole 50, I-95121 Catania, Italy

A. Terrasi, G. Franzó, and F. Priolo
INFM and Dipartimento di Fisica, Universitá di Catania, Corso Italia 57, I-95129 Catania, Italy
(Received 25 September 2003; revised manuscript received 8 January 2004; published 30 April 2004)

The local structure around Er^{3+} ions in Er+O doped silicon has been investigated by extended x-ray absorption spectroscopy. By comparing samples obtained by molecular-beam epitaxy and ion implantation a common structure comes out. Er is linked to five or six O atoms at around 2.24 Å and there is a well defined Er-O-Si bond angle of 135° and an Er-Si separation of 3.6 Å. The Er-Si distance is appreciably longer than that found in the more stable structures from *ab-initio* calculations and a discussion on the possible site for Er is presented.

DOI: 10.1103/PhysRevB.69.153310 PACS number(s): 61.72.Tt, 61.10.Ht, 78.55.Ap

I. INTRODUCTION

Er doped Si has been extensively studied in the recent years due to its potential application in optoelectronics.[1] The $^4I_{13/2} \rightarrow 4I_{15/2}$ transition, indeed, occurs at 1.54 μm, coinciding with one of the minimum absorption windows of commercial silica based optical fibers. The transition is forbidden by electrical dipole selection rules, but becomes possible whenever the Er ion is embedded in a noncentrosymmetric environment. This transition can be excited both optically[2] and electrically[3] in such systems. The major problem with the Er:Si system is the low solubility of this rare earth ion in the matrix, being of the order of 2×10^{16} Er/cm^2.[4] At this concentration theoretical calculations[5] find the tetrahedral interstitial site of the diamond structure (T_i) as the more probable site for Er. Experimental studies, based on the emission channelling technique,[6] have indeed found Er in the tetrahedral site. A successive investigation, based on the Zeeman effect on the 1.54 μm emission, has shown the presence of a well defined site for optically active Er centers with orthorhombic I(C_{2v}) symmetry.[7] However, this concentration level is unsuitable for the fabrication of devices. Using nonequilibrium techniques to raise the Er concentration above the solubility limit (namely, ion implantation), leads to the precipitation of Er in Er silicide form.[8,9] This compound, having cubic symmetry around the Er ion, produces no luminescence from the rare earth (RE). An efficient way to enhance the solubility of Er is in Si is the codoping with O. In this way Er binds to O ions and concentrations as high as 10^{19} Er/cm^3 can be incorporated in crystalline Si.[10] In samples with Er:O ratio equal to 1:10, strong luminescence at 1.54 μm has been observed at 77 K, with a moderate quenching as the temperature is increased up to room temperature.

In the case of Er+O doped system, theoretical studies exist proposing different sites for Er and its O cage in Si. In Ref. 11 the hexagonal interstitial site (H_i) is found to be the most stable, whereas in successive studies,[12,13] the T_i site is proposed for the ErO_6 complex. On the experimental side, electron paramagnetic resonance (EPR) studies[14,15] evidence two centers for the Er^{3+} ions: one of monoclinic symmetry having the rare-earth ion in a T_i site and one of trigonal symmetry with a RE ion in the middle of an H_i site or in an O decorated hexavacancy V_6 in the host crystalline Si. These findings are confirmed by recent Rutherford back-scattering (RBS) and channelling studies,[16] where coexistence of T_i and H_i sites is found, and the occurrency of Er in tetrahedral substitutional sites (T_s) is stated to be less than 5%.

The x-ray absorption fine structure (EXAFS) technique[17] has revealed to be effective in describing the local site of Er in crystalline Si,[8,9,18–20] amorphous hydrogenated Si (Refs. 21 and 22) and Si nanoparticles.[23] These studies, mainly based on the single scattering approximation for the data analysis,[17] show that Er is generally six coordinated to O ions at a distance of 2.24–2.26 Å. When Er is coordinated to less O ions,[21] the Er-O bond length shrinks to 2.09–2.14 Å. The use of the multiple scattering approximation on the other hand, revealed extremely effective in describing the site of Er and Yb beyond the O shell in glassy matrices like silicate[24,25] and phosphate[26] glasses.

The aim of this study was to determine the site of the Er ion in differently prepared Er+O doped crystalline Si samples by EXAFS. The results will be compared with the findings of theoretical calculations.

II. SAMPLE PREPARATION

Samples used for this study were prepared both by molecular beam epitaxy (MBE) and ion implantation (II) as resumed in Table I. MBE samples were grown onto (001) oriented Czochralsky Si wafers. Si evaporation, at a rate of 0.1 nm/s, was performed by electron gun in presence of an Er

TABLE I. Description of the preparation and thermal treatments of the samples used in the present investigations.

Sample	Method	Nominal molar ratio O/Er	Annealing temperature (°C)	Annealing time
33	MBE	1.8		
33C	MBE	1.8	900	1h
33D	MBE	1.8	1000	1h
33E	MBE	1.8	900	30s
49	MBE	5		
49C	MBE	5	900	1h
49D	MBE	5	1000	1h
49E	MBE	5	900	30s
145AD	II	10	900	12h
92AB	II	10	900	30s

flux arising from an effusion cell and a molecular oxygen leak into the MBE chamber. A pure Si buffer layer 100 nm thick was always deposited prior to the Er:O codoped layer, whose thickness was in the range 240–270 nm. The substrate temperature during the growth was kept at 550 °C, to ensure a good epitaxy, as always confirmed by in situ RHEED (reflection high-energy electron diffraction). With this technique, we have grown Si:Er:O layers with Er concentrations ranging in between 10^{19}–10^{20} Er/cm^{-3} and O in between $(1-2)\times10^{20}$ O/cm^{-3}. As far as the ion implantation (II) is concerned, samples were prepared by multiple implants of Er ($E_{impl}=0.5$–5 MeV) and O ($E_{impl}=0.15$–1.4 MeV) into (001) Si. In this way we produced a 2.3 μm thick amorphous layer with constant concentrations of 1×10^{19} Er/cm^3 and 1×10^{20} O/cm^3. After implantation, the samples underwent thermal processes at 900 °C for a short (30 s) and a long (12 h) time, to improve the crystalline quality and to promote the diffusion of O atoms around the Er sites.

III. EXPERIMENTAL DETAILS AND RESULTS

The experiments at the Er L_{III} edge were carried out at the GILDA CRG beamline at the European Synchrotron Radiation Facility. The sagittally focusing monochromator was equipped with a pair of Si(311) crystals, and used in dynamic focusing mode. Harmonic rejection was achieved by using a pair of Pd coated mirrors with an energy cutoff of 21 keV. The incoming beam was monitored by a nitrogen filled ion chamber, the absorption coefficient was measured by collecting the fluorescence yield from the samples using a 13 elements hyperpure Ge detector. In order to enhance the signals from far coordination shells, the measurements were carried out at liquid nitrogen temperature. two to four scans per sample were collected and averaged; powdered Er_2O_3 was collected in transmission mode as reference compound. A typical absorption spectrum is shown in Fig. 1 whereas an example of EXAFS spectrum with the relative fit is shown in Fig. 2. From the Fourier transform (inset of Fig. 1) it is evident the presence of a coordination peak just below 2 Å, due to the Er-O bond plus a further peak at 3.2 Å, that can be ascribed to an Er-Si coordination. Quantitative data analysis

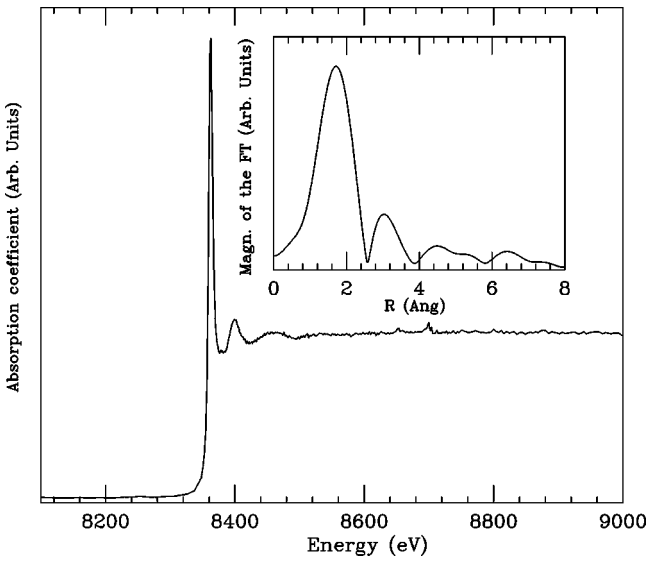

FIG. 1. Example of a typical measured absorption coefficient: sample 33*E*. The peaks due to Bragg scattering present in the spectrum at 8652 and 8699 eV were included in the background using the FITHEO code.[27] Inset: the Fourier transform of the EXAFS data of sample 33*E*. The transformation range was $k=2.4$–8.0 Å with a k^2 weight.

was carried out by using the GNXAS code.[27,28] The theoretical signals were calculated from a cluster derived from the crystalline structure of $Er_2Si_2O_7$.[29] Data were analyzed in the range $k=2.5$–9 Å^{-1} directly on the absorption spectrum. For the data analysis, we considered a model where each O around Er is linked to a Si atom. This is in agreement with the description of Er:O:Si complexes given in previous the-

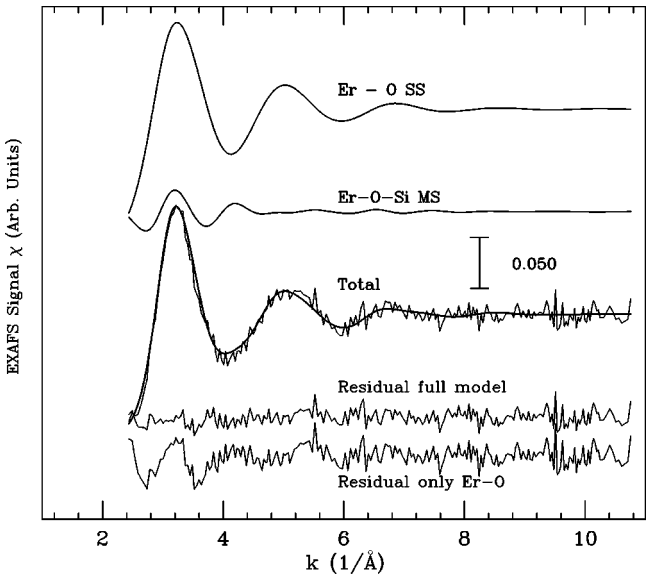

FIG. 2. Example of fit of a typical spectrum, sample 33*E*. The contributions from the Er-O and Er-O-Si atomic configurations are shown, as well as the experimental data and the total fit. The bottom curves shows the residual when using the full model or only the first Er-O shell. Note how, in the latter case, the residual strongly resembles the MS signal.

TABLE II. Results of the quantitative fits. For all spectra $R_{O-Si}=1.60$ Å, $\sigma^2_{Si-O}=0.0001$ Å^2 and $\sigma^2_{\Theta Er-O-Si}=30$ deg^2. Errors were determined by a χ^2 analysis with a confidence level of 95%.

Sample	N_{Er-O} ± 0.6	R_{Er-O} ± 0.02 Å	σ^2_{Er-O} ± 0.003 Å^2	$\Theta_{Er-O-Si}$ ± 4 deg	R_{Er-Si} ± 0.03 Å	σ^2_{Er-Si} ± 0.007 Å^2
33	5.7	2.22	0.015	134	3.55	0.020
33C	5.6	2.22	0.014	137	3.59	0.018
33D	5.7	2.23	0.012	135	3.62	0.014
33E	5.5	2.23	0.014	137	3.60	0.018
49	5.0	2.23	0.013	135	3.58	0.019
49C	5.8	2.22	0.016	136	3.58	0.018
49D	5.8	2.23	0.015	137	3.59	0.024
49E	4.8	2.24	0.013	136	3.59	0.017
145AD	5.5	2.23	0.012	138	3.62	0.019
92AB	5.9	2.25	0.015	136	3.63	0.021

oretical studies,[11–13] and can be parametrized with the following paths.

1. A single scattering (SS) Er-O path described by a bond length R_{Er-O} and Debye-Waller factor σ^2_{Er-O}.

2. A multiple scattering (MS) Er-O-Si path (including both the multiple scattering path and the Er-Si SS path) described by the first shell parameters plus the Si-O bond length R_{O-Si}, the Debye-Waller factor σ^2_{Si-O} and the angular parameters $\Theta_{Er-O-Si}$ and $\sigma^2_{\Theta Er-O-Si}$. The Er-Si bond length and Debye-Waller factors were derived from these data.

Each Er-O bond is associated to one Er-Si and one triangular Er-O-Si bonds. This comes from the fact that, being O bound to both Er and Si, a well defined Er-O-Si bond angle should exist as indeed found in glassy matrices.[24,26] In a geometrical picture, this also means that Er is linked to the SiO_4 tetrahedron by a corner. In the fitting procedure all the cited parameters plus the Er-O coordination number N_{Er-O} and the energy origin E_0 were varied with the exception of σ^2_{Si-O} (fixed to literature data $\sigma^2_{Si-O}=0.0001$ Å^2 Ref. 30), and the R_{O-Si} and $\sigma^2_{\Theta Er-O-Si}$ parameters, defined in the fit of sample 33*E* and then fixed for the others. The s_0^2 parameter was defined in the fit of the Er_2O_3 compound ($s_0^2=0.92$) and then kept fixed. The results are shown in Table II Other models were also tested, namely Er linked to a tetrahedron edge (2 Er-O-Si paths for 1 Er-Si path) or to a tetrahedron face (3 Er-O-Si paths for 1 Er-Si path), obtaining in all cases appreciably worse fits.

IV. DISCUSSION

First of all, it should be noted that all the samples exhibit the same local environment, despite of the different preparation conditions. This means that, by preparing the sample by MBE, an equilibrium configuration is attained already during the growth process and that successive thermal treatments have only minor effects on the local structure. Such structure is, moreover, the same obtained in ion implanted samples after a suitable annealing. Being II a markedly *nonequilibrium* technique, thermal treatments have, on the contrary, a noticeable effect, as shown in Ref. 9. In all samples, the RE appears to be five or six fold oxygen coordinated, with a bond length of 2.24 Å. The high Er-O coordination, present also in the sample with a nominal low O/Er ratio (Sample 33), could be ascribed to the diffusion of O species from the Czochralsky Si substrate. A similar effect has already been evidenced in literature.[8] A well defined Er-O-Si bond angle is found, of around 135°, leading to an Er-Si distance of 3.58 Å. The Er-O bond length falls in the typical range of previous EXAFS investigations.[8,9,18,20] A comparison with the existing theoretical predictions is provided in Table III. The first shell bond length R_{Er-O} is slightly longer than that calculated in the more stable structures in Refs. 11 and 12, whereas it results appreciably shorter that indicated for the T_i site in Ref. 13. More striking differences with the theoretical predictions are evident in the second coordination shell: here, the experimentally measured Er-Si separation (≈ 3.6 Å) is appreciably longer than that foreseen for the T_i or H_i sites, whereas it seems in a closer agreement with the Er-Si separations found in the T_s site. However, it must be noted that T_s is found to be the most stable site only in theoretical calculations for ErO_2 clusters,[13] and it is excluded by experimental studies like EPR (Refs. 14 and 15 or RBS.[16] A possible way to concile EXAFS data with the EPR and RBS studies is to consider the model proposed in Ref. 15. It consists of an Er ion in an H_i site sitting in the middle of a O decorated V_6 hexavacancy. *Ab initio* calculations[31] show that

TABLE III. Local structure parameters in a series of models proposed for the ErO_6 units in crystalline Si. In the case of Ref. 13 the data were derived from Fig. 3 of the paper. The asterisk (*) marks the phase indicated by the authors to be the more stable one.

Reference	Site	R_{Er-O}(Å)	R_{Er-Si}(Å)
11	T_i + O	2.47	2.51
11	T_s + O	2.18	3.86
11 (*)	H_i + O	2.18	2.60
12 (*)	T_i + O	2.17	3.05
13 (*)	T_i + O	2.45	2.89
13	T_s + O	2.38	3.33
13	T_s + O	2.20	3.33

such a vacancy is disk shaped, with a radius (center-to-silicon distance) of $R_v = 3.9$ Å, sufficient to allocate a central ErO_6 cluster. The Er-Si separation should be near R_v so compatible, considering possible relaxation, with our data.

V. CONCLUSION

In this work we have studied the local structure around Er^{3+} ions in Er+O doped crystalline Si, by means of EXAFS. Data analysis evidenced that erbium is bound to O atoms at 2.24 Å and that there is a well defined Er-O-Si bond angle of about $\approx 135°$ and an Er-Si separation of ≈ 3.60 Å. The results are compared with the findings of theoretical calculations, evidencing that a too short Er-Si distance is in general foreseen in the proposed structures. On the other hand, structures based on Er sitting inside O-decorated hexavacancies appear to be in agreement with our findings.

*Electronic address: dacapito@esrf.fr
†Also at INFN, Laboratori Nazionali di Frascati, P.O. Box 13, I-00044 Frascati (Roma), Italy.

[1] *Rare Earth Doped Semiconductors II*, edited by S. Coffa, A. Polman, and R.N. Schwartz, Mater. Res. Soc. Symp. Proc. No. 402 (Materials Research Society, Pittsburgh, 1996).
[2] S. Coffa, F. Priolo, G. Franzo, V. Bellani, A. Carnera, and C. Spinella, Phys. Rev. B **48**, 11 782 (1993).
[3] G. Franzo, F. Priolo, S. Coffa, A. Polman, and A. Carnera, Appl. Phys. Lett. **64**, 2235 (1994).
[4] F.Y.G. Ren, J. Michel, Q. Sun-Paduano, B. Zheng, H. Kitagawa, D.C. Jacobson, and J.P.L.C. Kimlerling, in *Rare Earth Doped Semiconductors*, edited by G.S. Pomrenke, P.B. Klein, and D.W. Langer, Mater. Res. Soc. Symp. Proc. No. 301 (Materials Research Society, Pittsburgh, 1993).
[5] M. Needels, M. Schluter, and M. Lannoo, Phys. Rev. B **47**, 15 533 (1993).
[6] U. Wahl, A. Vantomme, J. DeWachter, R. Moons, G. Langouche, J.G. Marques, and J.G. Correia, Phys. Rev. Lett. **79**, 2069 (1997).
[7] N.Q. Vinh, H. Przybylinska, Z.F. Krasil'nik, and T. Gregorkiewicz, Phys. Rev. Lett. **90**, 066401 (2003).
[8] D.L. Adler, D.C. Jacobson, D.J. Eaglesham, M.A. Marcus, J.L. Benton, J.M. Poate, and P.H. Citrin, Appl. Phys. Lett. **61**, 2181 (1992).
[9] A. Terrasi, G. Franzo, S. Coffa, F. Priolo, F. d'Acapito, and S. Mobilio, Appl. Phys. Lett. **70**, 1712 (1997).
[10] S. Coffa, G. Franzo, F. Priolo, A. Polman, and R. Serna, Phys. Rev. B **49**, 16 313 (1994).
[11] J. Wan, Y. Ling, Q. Sun, and X. Wang, Phys. Rev. B **58**, 10 415 (1998).
[12] M. Hashimoto, A. Yanase, H. Harima, and H. Katayama-Yoshida, Physica B **308-310**, 378 (2001).
[13] A.G. Raffa and P. Ballone, Phys. Rev. B **65**, 121309 (2002).
[14] J.D. Carey, R.C. Barklie, J.F. Donegan, F. Priolo, G. Franzo, and S. Coffa, Phys. Rev. B **59**, 2773 (1999).
[15] J.D. Carey, J. Phys.: Condens. Matter **14**, 8537 (2002).
[16] M.B. Huang and X.T. Ren, Phys. Rev. B **68**, 033203 (2003).
[17] P.A. Lee, P.H. Citrin, P. Eisenberger, and B.M. Kincaid, Rev. Mod. Phys. **53**, 769 (1981).
[18] M. Ishii, T. Ishikawa, T. Ueki, S. Komuro, T. Morikawa, Y. Aoyagi, and H. Oyanagi, J. Appl. Phys. **85**, 4024 (1999).
[19] A. Terrasi, F. Priolo, G. Franzo, S. Coffa, F. d'Acapito, and S. Mobilio, J. Lumin. **80**, 363 (1999).
[20] S. Pizzini, S. Binetti, D. Calcina, N. Morgante, and A. Cavallini, Mater. Sci. Eng., B **72**, 173 (2000).
[21] C. Piamonteze, A.C. Iniguez, L.R. Tessler, M.C.M. Alves, and H. Tolentino, Phys. Rev. Lett. **81**, 4652 (1998).
[22] L.R. Tessler, C. Piamonteze, M.C. Martins Alves, and H. Tolentino, J. Non-Cryst. Solids **266-269**, 598 (2000).
[23] L.R. Tessler, J.L. Coffer, J. Ji, and R.A. Senter, J. Non-Cryst. Solids **299-302**, 673 (2002).
[24] F. d'Acapito, S. Mobilio, P. Gastaldo, D. Barbier, L.F. Santos, O. Martins, and R.M. Almeida, J. Non-Cryst. Solids **293-295**, 118 (2001).
[25] F. d'Acapito, S. Mobilio, L. Santos, and R.M. Almeida, Appl. Phys. Lett. **78**, 2676 (2001).
[26] F. d'Acapito, S. Mobilio, P. Bruno, D. Barbier, and J. Philipsen, J. Appl. Phys. **90**, 265 (2001).
[27] A. Filipponi and A. Di Cicco, Phys. Rev. B **52**, 15 135 (1995).
[28] A. Filipponi, A. Di Cicco, and C.R. Natoli, Phys. Rev. B **52**, 15 122 (1995).
[29] Y.I. Smolin and Y.F. Shepelev, Acta Crystallogr., Sect. B: Struct. Crystallogr. Cryst. Chem. **26**, 484 (1970).
[30] G.N. Greaves, A. Fontaine, P. Lagarde, D. Raoux, and S.J. Gurman, Nature (London) **293**, 611 (1981).
[31] J.L. Hastings, S.K. Estreicher, and P.A. Fedders, Phys. Rev. B **56**, 10 215 (1997).